

Disruption of corticocortical information transfer during ketamine anesthesia in the primate brain

Karen E. Schroeder^a, Zachary T. Irwin^a, Matt Gaidica^b, J. Nicole Bentley^c, Parag G. Patil^{a,c,d}, George A. Mashour^{b,e,f,1}, Cynthia A. Chestek^{a,b,e,g,h,*,1}

^a Department of Biomedical Engineering, University of Michigan, Ann Arbor, MI 48109, United States

^b Neuroscience Graduate Program, University of Michigan Medical School, Ann Arbor, MI 48109, United States

^c Department of Neurosurgery, University of Michigan Medical School, Ann Arbor, MI 48109, United States

^d Department of Neurology, University of Michigan Medical School, Ann Arbor, MI 48109, United States

^e Center for Consciousness Science, University of Michigan Medical School, Ann Arbor, MI 48109, United States

^f Department of Anesthesiology, University of Michigan Medical School, Ann Arbor, MI 48109, United States

^g Department of Electrical Engineering and Computer Science, University of Michigan, Ann Arbor, MI 48109, United States

^h Department of Robotics, University of Michigan, Ann Arbor, MI 48109, United States

ARTICLE INFO

Article history:

Received 29 November 2015

Revised 9 April 2016

Accepted 15 April 2016

Available online 16 April 2016

Keywords:

Consciousness

Ketamine

Anesthesia

Sensorimotor

Functional connectivity

Information integration

ABSTRACT

The neural mechanisms of anesthetic-induced unconsciousness have yet to be fully elucidated, in part because of the diverse molecular targets of anesthetic agents. We demonstrate, using intracortical recordings in macaque monkeys, that information transfer between structurally connected cortical regions is disrupted during ketamine anesthesia, despite preserved primary sensory representation. Furthermore, transfer entropy, an information-theoretic measure of directed connectivity, decreases significantly between neuronal units in the anesthetized state. This is the first direct demonstration of a general anesthetic disrupting corticocortical information transfer in the primate brain. Given past studies showing that more commonly used GABAergic drugs inhibit surrogate measures of cortical communication, this finding suggests the potential for a common network-level mechanism of anesthetic-induced unconsciousness.

© 2016 Published by Elsevier Inc.

1. Introduction

Most clinically-used general anesthetics act by potentiating the transmission of γ -aminobutyric acid (GABA), leading to depression of neuronal function and conscious processing (Alkire et al., 2008). Ketamine, however, does not depress the cortex and fails to conform to most mechanistic frameworks of general anesthesia: it does not bind with high affinity to the GABA_A receptor (Antkowiak, 1999; Salmi et al., 2005), depress thalamic metabolism (Långsjö et al., 2005), activate the sleep-promoting ventrolateral preoptic nucleus (Lu et al., 2008), or depress high-frequency electroencephalographic activity (Lee et al., 2013). Identifying common neural features of ketamine and GABAergic anesthetics would therefore be an important step toward a foundational understanding of anesthetic-induced unconsciousness. We have recently demonstrated in human surgical patients that ketamine, like the GABAergic drugs propofol and sevoflurane, depresses

directed connectivity across frontal–parietal networks (Lee et al., 2013; Blain-Moraes et al., 2014). However, these and other electroencephalogram (EEG)- (Ferrarelli et al., 2010; Casali et al., 2013) and fMRI-based (Schrouff et al., 2011) connectivity studies of large-scale brain networks are based upon an assumption that the measured activity actually reflects information transfer along corticocortical pathways. A more direct measurement of functional connectivity of neurons and information integration is essential to validate these data.

In the current study, we used intracortical multi-electrode arrays in the *Macaque* brain to more directly observe sensory information being shared between primary somatosensory cortex (S1, area 3b) and primary motor cortex (M1, area 4), two regions that communicate bidirectionally via local circuits through areas 1, 2 and 5 (Jones et al., 1978). We provided passive stimulation to the fingers of two monkeys (Fig. 1A), and recorded neural data from M1 and S1 before, during, and after ketamine-induced unconsciousness. We used a purely somatosensory, 2 Hz rhythmic stroking stimulation of the glabrous finger pads, which are quite sensitive to light touch. Along with S1, neurons in monkey M1 (particularly those in the most posterior region) are responsive to purely tactile stimulation of the digits, as well as passive movement (Fetz et al., 1980; Lemon, 1981; Tanji and Wise, 1981).

* Corresponding author at: 2800 Plymouth Rd. Building 10 Room A171; Ann Arbor, MI 48105, United States.

E-mail address: cchestek@umich.edu (C.A. Chestek).

¹ These authors contributed equally to this work.

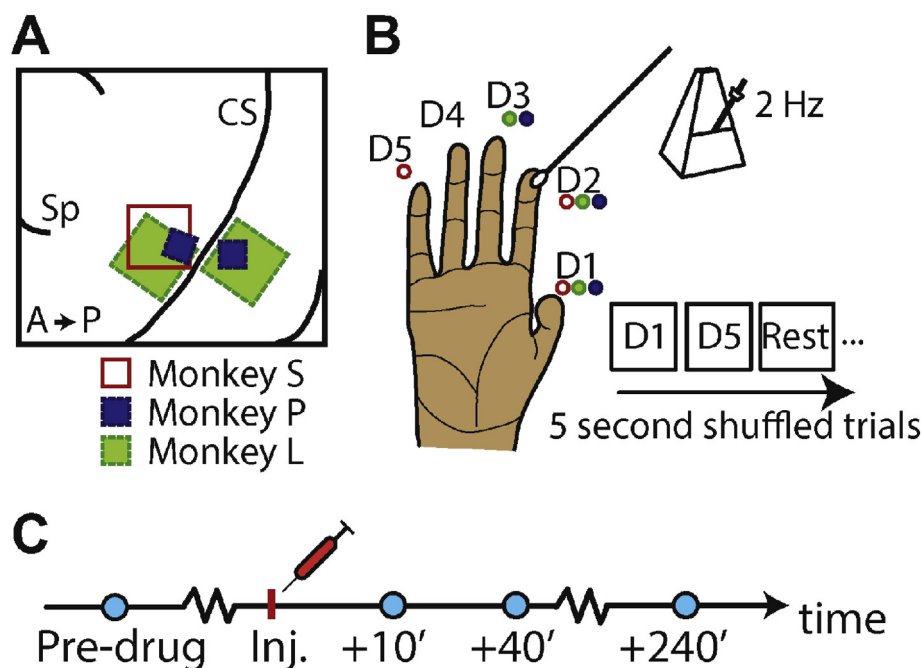


Fig. 1. (A) Electrode placement in three monkeys. A: anterior; P: posterior; CS: central sulcus; Sp: spur of the arcuate. (B) Experimental trial structure and digits stimulated on each animal — color legend same as (A). (C) Trial block structure for each day of experiments. Blue marker denotes block of stimulation trials. Inj: intramuscular ketamine injection.

2. Materials & methods

All procedures were carried out in accordance with protocols approved by the University Committee on Use and Care of Animals at the University of Michigan.

2.1. Surgery and experimental structure

Three rhesus macaques were implanted with multielectrode arrays in motor and sensory cortices, as diagrammed in Fig. 1A. In Monkey P, data were recorded from two 2.5 mm × 1.95 mm 16-channel Floating Microelectrode Arrays (FMAs, Microprobes), one of which was placed in finger area of M1, and the other placed in finger area of S1. In Monkey L, data were recorded from two 4 mm × 4 mm 96-channel Utah Arrays (Blackrock Microsystems), one of which was placed in finger area of M1, and the other placed in finger area of S1. In Monkey S, data were recorded from one 4 mm × 4 mm 96-channel Utah Array (Blackrock Microsystems) implanted in finger area of M1. The arrays were placed by first locating the point at which a line projecting from the genu of the arcuate sulcus would intersect central sulcus. The M1 array was placed at this location, just anterior to central sulcus. The S1 arrays were placed across from it, just posterior to central sulcus. Given the placement, size, and electrode length (1.5 mm for Utah, 1.0–4.5 mm for FMA) of the S1 arrays, a Rhesus atlas (Saleem and Logothetis, 2012) predicted that the majority of the recording sites would fall in Brodmann area 3b, although it is possible that a small minority, particularly in monkey P, were located in area 1.

We trained the three monkeys over the course of several weeks to sit quietly in a chair (Crist Instruments) using small juice rewards. Animals' heads remained secured to the chair and motionless during all training and experiments with a titanium post (Crist Instruments) embedded in the head cap. The hand contralateral to the implant was immobilized against an acrylic plate, and a cotton-tipped applicator was used to stroke the appropriate finger pad at 2 Hz, as timed by a metronome (Fig. 1B). Once monkeys were sufficiently trained, they each participated in 1 or 2 days of experiments with anesthesia. The time course of an experiment is shown in Fig. 1C. Animals remained connected to the data

acquisition system continuously for the first three time points to enable tracking of multiunits and oscillations over time. Monkey S is the exception to this, and only participated in an abbreviated experiment with two time points. At least two weeks were allowed between experiments for a given animal to minimize stress due to the experimental protocol.

2.2. Neural recording

A computer running xPC Target (Mathworks) cued the experimenter and synchronized behavioral and neural data for analysis. Trials were randomized and interspersed with rest trials, each lasting 5 s. The stimuli were entirely passive; if the monkey moved during any trial, it was flagged as invalid by an observing experimenter and not used in subsequent analysis. For monkey L experiments, the applicator was instrumented with a triple axis analog accelerometer (SparkFun) to better align behavioral and neural data.

Broadband neural data was sampled at 30 kHz and recorded using a Cerebus neural signal processor (NSP, Blackrock Microsystems). Collected data were processed and analyzed in three forms: 30 kHz broadband was saved and subsequently decomposed into frequency bands (see Section 2.5), thresholded unit activity was obtained by thresholding at −4.5 times the RMS voltage on each channel (see Section 2.4), and multiunit activity was hand sorted using Plexon Offline Sorter. The data collected from each animal is summarized in Table 1.

Table 1
Summary of collected data.

	Monkey L	Monkey P	Monkey S
# Experiments	2	2	1*
Implant(s)	M1 + S1, Utah	M1 + S1, FMA	M1 Utah
# Electrodes M1/S1	64/64**	16/16	96/0
# Multiunits M1/S1	94/37	17/18	50/0
# Trials per time point	48–66	30–65	40–75

* Only pre-drug and +:10 time points collected.

** Only 64 channels from each array were recorded simultaneously.

Table 2
Observations of anesthetic depth.

Test	+ 10 minutes	+ 40 minutes	+ 240 minutes
Spontaneous movement	None	Occasional facial or hand movement	Normal movement of limbs, face and torso
Pedal reflex	No movement	Minimal response, if any; some digit flexion	Strong withdrawal
Blink reflex	No movement	Occasional weak blinking	Normal blinking
Limb manipulation	No response when handled	Minimal response; some digit flexion	Limb withdrawn when handled
Vertical nystagmus	Present	Present	Not present

2.3. Anesthesia

Ketamine was administered once per experiment as a 10 mg/kg intramuscular injection to the upper thigh while the animal was seated in a chair. Arousal was monitored at least every 15 min until the animal was fully responsive, particularly before each set of experimental trials. The metrics of arousal used were vertical nystagmus, pedal (toe pinch) reflex, blink reflex, limb manipulation (picking up arm or leg and allowing to fall into experimenter's hand), and spontaneous movements. Although ketamine levels in the blood were not monitored, anesthetic effects seen at each time point were common to all animals, and are described in Table 2. Due to the one-time administration of the drug, the level of anesthesia was not identical at the different time points; indeed, the goal was to investigate features of the neural signal in different states.

2.4. Data analysis – spikes

A Naive Bayes decoder with leave-one-out cross-validation was used to classify the location of the stimulus on a given trial. The inputs to the decoder were the firing rates of either thresholded activity or hand-sorted multiunits during the center 3 s of each trial. The beginning and end of each trial were excluded to avoid the periods of time when the experimenter was switching between fingers. Only three fingers per animal were used in order to increase the number of trials completed per finger, given the time constraints of the anesthesia. The particular fingers used for each monkey were chosen during a separate session of awake stimulation. The fingers with the greatest number of channels responsive to stimulation, as compared with a rest condition, were used for subsequent experiments. Only modulated thresholded channels or multiunits were used; modulation was determined with an ANOVA ($\alpha = .05$) of firing rates during the different finger conditions. Chance level was 33.3% for a 1 of 3 choices, and the decoder could not perform better by choosing the most common condition, as the number of trials per finger condition were always balanced. Percent correct at each time point was tested for significance versus chance with a one-sided one-sample z-test. The number of datasets used for decoding from each brain area were 5 for M1 (3 animals) and 4 for S1 (2 animals).

The power spectrum for each multiunit was computed using the center 3 s of each trial, split into 1 ms bins. These binned spike trains were then converted to a spike density function (SDF) by convolution with a Gaussian kernel ($\sigma = 15$ ms). The power spectra of the SDFs were then computed with Matlab's discrete Fourier transform, *fft*. The spectra of all units for all trials were then averaged together and normalized by the peak power, which occurred between 0 and 1 Hz. Data for this analysis were taken from two monkeys (P and L), who each completed two experiments.

High order transfer entropy (HOTE) was computed using the Transfer Entropy Toolbox for Matlab (Ito et al., 2011). Data for this analysis were taken from two monkeys (P and L), who each completed two experiments. Data were prepared by taking multiunit sorted spike trains, extracting spike times during the center 3 s of each trial (the same portions as used for decoding), and concatenating them to form one vector per multiunit per experiment with length between 3 and 6 min. Equal numbers of awake and ketamine trials were used for

each experiment. Spikes were then binned in 1 ms bins and passed to the toolbox, which calculated HOTE for each possible multiunit pair. All entropies were 5th order, with possible time lags of 1 to 30 ms. Only the peak, or maximum, value for each multiunit pair over all possible time lags was included in plots. For shuffled HOTE, S1 spike trains were shuffled using Matlab's *randperm* before calculating peak HOTE for each pair.

2.5. Data analysis – oscillations

The recording sessions from monkeys L and P were split into 5 s bins where the signal was free from high amplitude artifacts, and then power spectra were created for each bin using MATLAB's *fft* function. Power at 1 Hz increments (1–4 Hz for delta, 13–30 Hz for beta, and 40–80 Hz with 59–61 Hz excluded for gamma) was calculated and then averaged

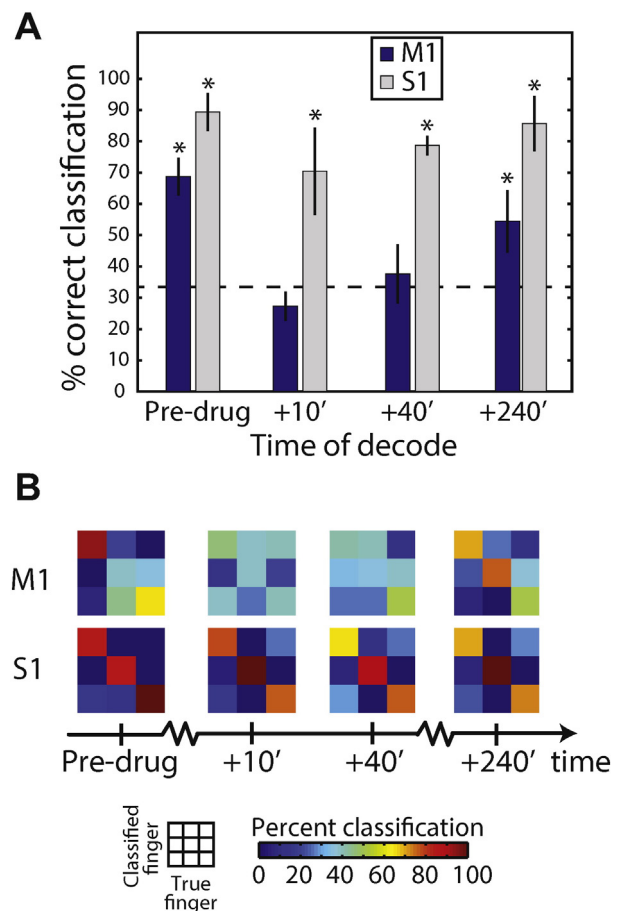


Fig. 2. Loss of sensory representation from motor cortex under ketamine. (A) Percent correct classification of stimulated finger across all monkeys and sessions. * $p < .001$ when compared to chance level (dashed line). Error bars denote S.E.M. (B) Example confusion matrices showing decoder performance for one session of Monkey P.

together in 1 min increments over 100 min of the experiment. Power on all electrodes was averaged together, smoothed with a window size of 10, and normalized by dividing by average power over the entire 1–80 Hz band. Example spectrograms (Fig. 5B) represent single electrode activity from a single experiment with monkey L. The Chronux toolbox for Matlab was used to generate the spectrogram plots after data were decimated and bandpass filtered between 0 and 80 Hz.

3. Results

3.1. Loss of cortical sensory information transfer during ketamine exposure

Before ketamine administration, the identity of the stimulated finger could be correctly classified from thresholded neural activity on the M1 and S1 electrodes (Fig. 2A) using a Naïve Bayes decoder, with a mean accuracy of 68.7% from M1 electrodes and 89.3% from S1 electrodes. After an intramuscular injection of ketamine (10 mg/kg), animals reached unconsciousness within 10 min, as judged by lack of pedal and eye blink reflexes. From 10 to 30 min post-injection, while animals were completely unresponsive, decoding performance from M1 decreased to chance levels (Fig. 2A), with a mean of 27.4% correct. The consistency of the stimulus in monkey L was verified with stimulator-mounted accelerometers; no difference in the number of strokes before or after ketamine was found on either day ($p = .67/p = .26$, t-test). At 4 h post-injection, when consciousness had returned, M1 decodes recovered to 54.4% correct, significantly above chance. Importantly, even when M1 decodes were disrupted, S1 decodes did not significantly decrease. This result is consistent with the hypothesis that, during exposure to ketamine, sensory information can still reach S1 from the thalamus, but is prevented from reaching M1 via an interruptible corticocortical pathway. It should be noted that surrogates of preserved primary sensory processing, such as somatosensory-evoked potentials and intra-network connectivity of primary sensory cortex, have been observed during unconsciousness induced by GABAergic anesthetics in humans (Banoub et al., 2003; Boveroux et al., 2010).

In addition to ensemble representation, the behavior of hand-sorted multiunits was analyzed (see Materials & methods). Decodes performed with multiunits followed the same pattern as thresholded data, with a mean percent correct classification of 52.5% correct from M1 and 74.84% correct from S1 while awake, decreasing to 26.12% (chance level) and 68.69% respectively at 10 min post-injection, and finishing at 49.15% and 76.28% after 4 h. Lower percentages than those achieved with thresholded data were expected, considering the small number of well-isolated units compared with the number of unsortable channels with clear bipolar activity. Mean firing rates remained stable among M1 and S1 multiunits (Fig. 3A): while some cells increased and others decreased their firing rate, paired t-tests revealed no significant changes in overall firing rates in any animal, after correcting for multiple tests. Examples of unit responses are shown in Fig. 3B and C, with stimulus-aligned bursting activity shown for several M1 units. The presence of a 2 Hz peak (the frequency of stimulation) in the power spectra of M1 and S1 single unit spike trains (Fig. 3D) followed the pattern of decoding performance, disappearing in M1 units under ketamine anesthesia and recovering at the final time point. The magnitudes of the peaks from pre-normalized S1 unit spectra did not change significantly (paired t-test, $\alpha = .05$) from pre-drug to 10 min post-injection.

3.2. Loss of functional connectivity during ketamine exposure

Knowing that M1 and S1 have reciprocal, though not necessarily monosynaptic, corticocortical connections (Jones et al., 1978), we

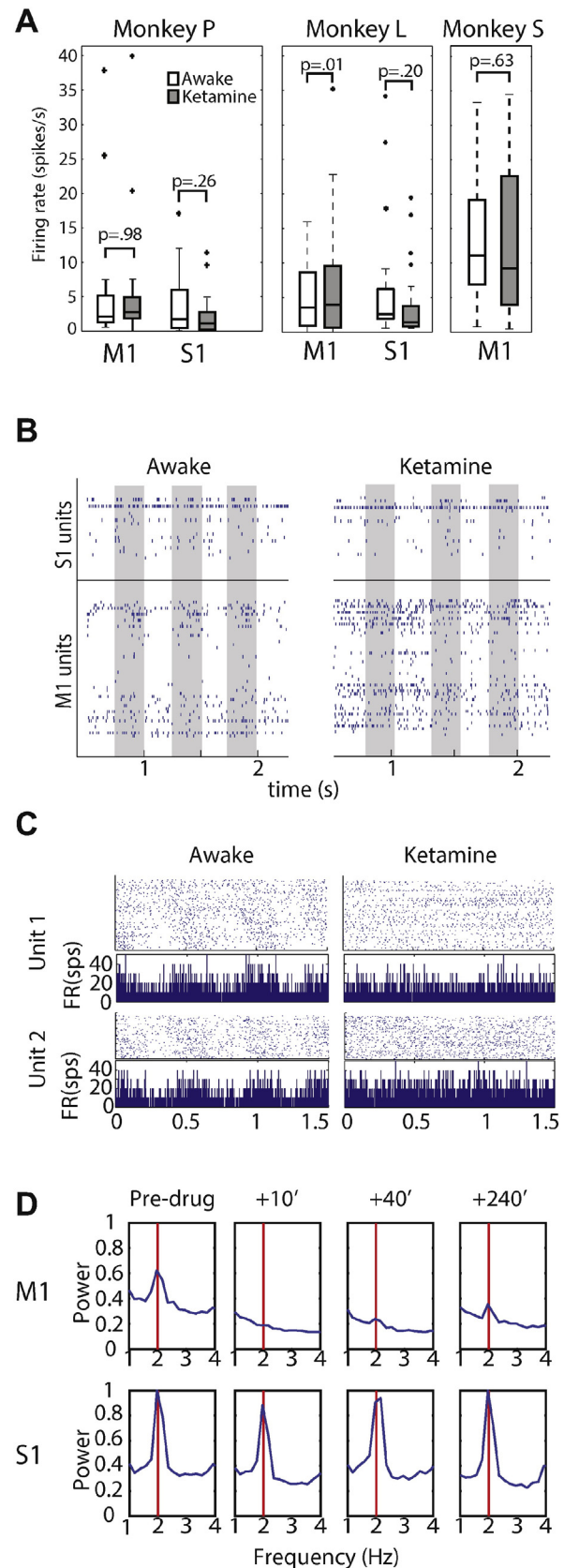


Fig. 3. Multiunit behavior and power spectra. (A) Firing rates of sorted multiunits before and after ketamine (+10' time point). (B) Example raster plot of all recorded multiunits during portions of one awake trial and one ketamine trial from monkey L. Gray bars: stimulator in contact with digit. (C) PSTHs of two example M1 units, aligned to first stimulus of trial. (D) Normalized mean power spectra for unit activity averaged across modulated units from monkeys P and L. Red vertical line emphasizes 2 Hz, the frequency of stimulation. (For interpretation of the references to color in this figure legend, the reader is referred to the web version of this article.)

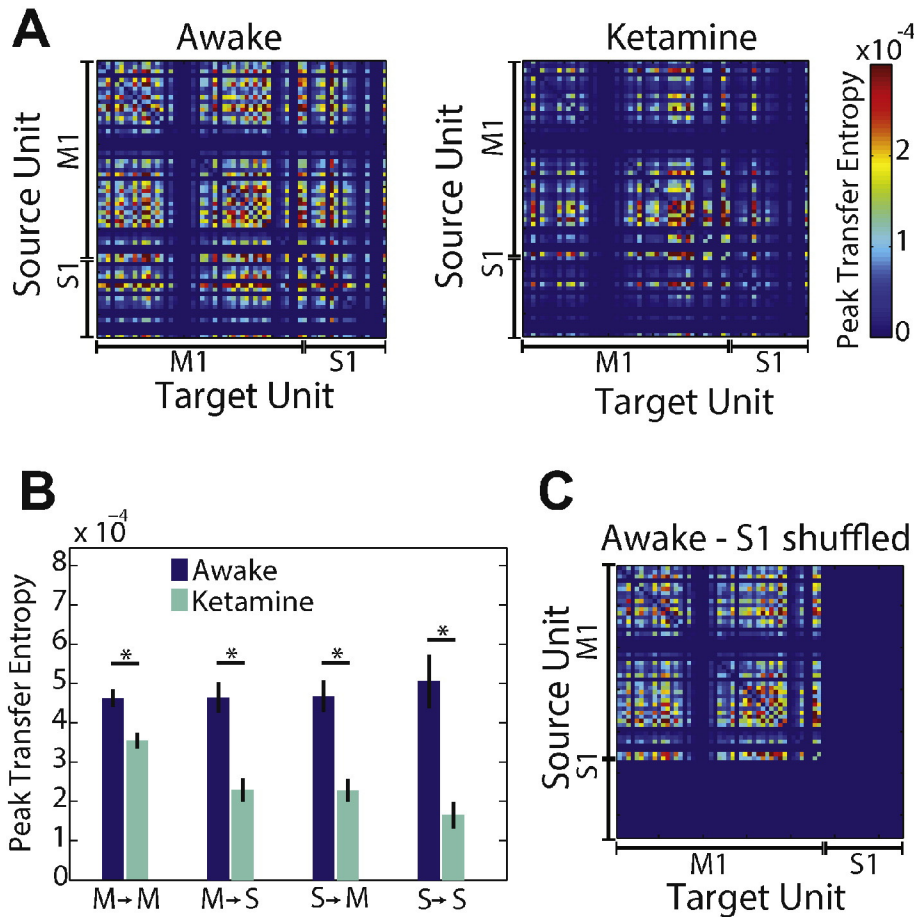


Fig. 4. Loss of corticocortical directed connectivity under ketamine. (A) Peak high order transfer entropy (HOTE) between multiunit pairs during one monkey L experiment. (B) Comparison of Peak HOTE including all sessions for monkeys P and L. $*p < .001$. (C) HOTE between multiunit pairs after shuffling S1 spikes; same dataset as (A).

investigated whether the disappearance of M1 representation could be explained by a loss of functional connectivity between the two regions. We applied high order transfer entropy (HOTE), an information-theoretic measure of directed connectivity between neurons (Ito et al., 2011), to multiunit spike trains from monkeys L and P. HOTEs were computed for each possible multiunit pair during a given recording session. Inter-region connectivity decreased significantly for combined monkey sessions (Fig. 4B) as well as for each individual session (all paired t-tests, $\alpha = .05$, $n = 1889$ total M1/S1 pairs). These results support the observation of reduced information transfer between the two cortical regions under ketamine. Intra-areal S1 HOTE also decreased, which was not necessarily expected, given its sustained sensory representation. This reflects a decrease in the ability of S1 neurons to help predict each other's behavior in general, which may indicate a larger change in S1 firing behavior beyond task-relevant information transfer.

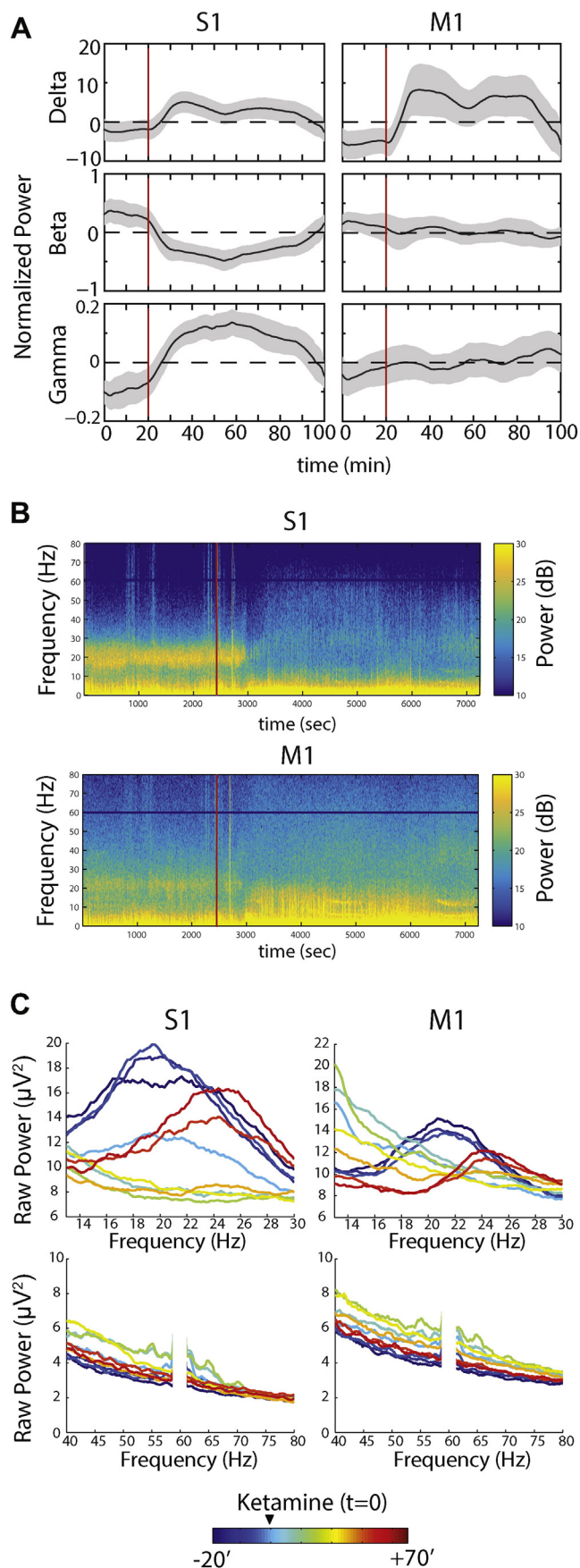
3.3. Spectral changes during ketamine exposure

Finally, we investigated changes in neural oscillations that could potentially explain the observed cortical disconnection. S1 exhibited changes in oscillatory activity that were time-locked with the administration of ketamine and correlated with the conscious state of the monkey (Fig. 5A–C). Relevant modulations in the delta (1–4 Hz), beta (15–30 Hz) and gamma (40–80 Hz) bands were observed in S1 in both monkeys (Fig. 5 and S2). Modulations in M1 were smaller and less visible when averaging across all electrodes, but were similar to S1 on select electrodes (Fig. 5C and S2). These data are directly

homologous to our EEG observations in humans (Lee et al., 2013) during ketamine-induced unconsciousness, and suggest that the monkeys were in a comparable state of clinical anesthesia.

4. Discussion

We have demonstrated that (1) thalamocortical information transfer and primary sensory representation persist during ketamine anesthesia, as evidenced by the preserved ability to decode tactile stimuli in S1; (2) information transfer is disrupted between S1 and M1 during ketamine anesthesia, as evidenced by the inability to decode tactile stimuli in M1; (3) transfer entropy, a surrogate for information exchange, is disrupted between neuronal units in S1 and M1; and (4) in S1, beta oscillations are suppressed while gamma and delta oscillations are augmented, as found with scalp EEG during ketamine anesthesia in humans. This experimental paradigm represents the most compelling evidence to date for reduced cortical information transfer and the inter-areal unbinding of cortical representations in the anesthetized state (Mashour, 2013). One potential concern with this interpretation is the possibility that somatosensory information may be reaching M1 directly from thalamus, which would allow the possibility of a thalamocortical rather than a corticocortical breakdown of information exchange. However, according to the literature, the thalamus does not send M1 information about tactile sensation, but rather only proprioception and other movement-related parameters (Rizzolatti and Luppino, 2001; Shipp, 2005). Regardless, the cortical connections between M1 and S1 are of primary interest here. Somatosensory stimulation is known to elicit both short- and long-latency



evoked potentials in S1, with the long-latency responses attributed to corticocortical communication. It is these late responses that are normally associated with conscious awareness of a stimulus (Caulier and Kulics, 1991; Supér et al., 2001; Del Cul et al., 2007) and selectively suppressed under anesthesia in S1 and primary visual cortex (V1) (Banoub et al., 2003; Hudetz et al., 2009). These late evoked responses are sometimes thought of as “top-down” processes, as they involve re-entrant communication from areas higher in the cognitive hierarchy, such as association cortices. In the case of S1, motor areas are the source of some important top-down communication: Manita et al. (2015) showed that long-latency inputs from M2 to S1 in the mouse were critical for accurate sensory perception. Taken together, the data support a top-down mechanism for accurate perceptual representation, where reciprocal corticocortical connections are necessary for conscious experience (Mashour, 2014).

Although disrupted cortical information transfer may represent a proximate cause for unconsciousness, the root cause of communication breakdown remains just as uncertain as the details of the communication itself. Top-down sensory processing necessitates coordination across distributed populations, a complex task that is almost certainly driven by oscillatory activity (Engel et al., 2001; Bressler and Richter, 2015). Low beta in particular, where we saw the most modulation, is relevant to top-down synchrony (Bressler and Richter, 2015), though we did not see significant modulations in M1. Beta oscillations have previously been implicated as information carriers in the sensorimotor system: synchronous beta activity in motor cortex appears to mediate directionally-specific information flow (Rubino et al., 2006), and postcentral beta causally influences precentral beta (Brovelli et al., 2004). Conversely, gamma oscillations may mediate bottom-up, or feed-forward, sensory processing (Bressler and Richter, 2015), perhaps providing local gain on subsets of neurons (Pritchett et al., 2015). It is unclear whether our observed increase in gamma indicates an attempt at communication, or is simply the response of a circuit that has become disconnected and unbalanced. As for the origins of these waves, evidence supports the thalamus as responsible for overall control over cortical oscillations (Jones, 2001; Saalmann, 2014), and our data are consistent with the temporal binding model, where thalamocortical circuits synchronize cortical networks, modifying and enhancing cortical inputs to enable sensory awareness. Although the precise thalamic population responsible is unknown, ketamine is known to modulate normal thalamic function in general, as evidenced by increased glucose metabolism (Långsjö et al., 2005). Simultaneous cortical and thalamic recordings could potentially clarify these issues.

In summary, we have shown evidence for intact first-order thalamocortical information transfer to S1 during ketamine anesthesia and, through oscillatory behavior, indirect evidence for a higher-order thalamic influence on S1 that might account for the reduced transfer entropy of S1–M1 neuronal pairs that are functionally coupled in the waking state. The fact that this was demonstrated with the anesthetic ketamine is even more striking considering its unique traits at the molecular and systems neuroscience level. This direct demonstration of disrupted corticocortical information transfer, along with accumulating evidence for reduced surrogates of cortical communication during GABAergic anesthesia in humans (Ferrarelli et al., 2010; Casali et al., 2013; Lee et al., 2013), suggest a common final pathway for unconsciousness induced by molecularly distinct anesthetics. It should be noted, however, that spectral changes and depression of directed and effective connectivity can also be observed at subanesthetic doses of ketamine in humans (Lee et al., 2013; Muthukumaraswamy et al.,

Fig. 5. S1 electrodes lose beta power, gain gamma under ketamine. (A) Band power modulations of two monkey P sessions and two monkey L sessions (shaded area: SD, red vertical bar: injection). (B) Spectrograms from representative electrodes in S1 and M1 during a single Monkey L session (red vertical bar: injection). (C) Raw beta and gamma power from representative electrodes in S1 and M1 during a single monkey L session. (For interpretation of the references to color in this figure legend, the reader is referred to the web version of this article.)

2015; Rivolta et al., 2015). Further work is required to assess whether functional disconnections in the cortex are epiphenomenal to general anesthesia or are dose-dependently reduced to a critical threshold that causes the anesthetized state.

Acknowledgments

We would like to thank Kaile Bennett for animal training and care, Autumn Bullard, David Thompson, and Derek Tat for assistance with data collection, Adam Sachs for surgical assistance with monkey S, and Paras Patel for assistance with data processing. This work was supported by the National Institutes of Health, Bethesda, MD, USA (grant R01GM111293).

Appendix A. Supplementary data

Supplementary data to this article can be found online at <http://dx.doi.org/10.1016/j.neuroimage.2016.04.039>.

References

- Alkire, M.T., Hudetz, A.G., Tononi, G., 2008. Consciousness and anesthesia. *Science* 322, 876–880.
- Antkowiak, B., 1999. Different actions of general anesthetics on the firing patterns of neocortical neurons mediated by the GABA(A) receptor. *Anesthesiology* 91, 500–511.
- Banoub, M., Tetzlaff, J.E., Schubert, A., 2003. Pharmacologic and physiologic influences affecting sensory evoked potentials: implications for perioperative monitoring. *Anesthesiology* 99, 716–737.
- Blain-Moraes, S., Lee, U., Ku, S., Noh, G., Mashour, G.A., 2014. Electroencephalographic effects of ketamine on power, cross-frequency coupling, and connectivity in the alpha bandwidth. *Front. Syst. Neurosci.* 8, 114.
- Boveroux, P., Vanhaudenhuyse, A., Bruno, M.-A., Noirhomme, Q., Lauwrick, S., Luxen, A., Degueldre, C., Plenevaux, A., Schnakers, C., Phillips, C., Brichant, J.-F., Bonhomme, V., Maquet, P., Greicius, M.D., Laureys, S., Boly, M., 2010. Breakdown of within- and between-network resting state functional magnetic resonance imaging connectivity during propofol-induced loss of consciousness. *Anesthesiology* 113, 1038–1053.
- Bressler, S.L., Richter, C.G., 2015. Interareal oscillatory synchronization in top-down neocortical processing. *Curr. Opin. Neurobiol.* 31, 62–66.
- Brovelli, A., Ding, M., Ledberg, A., Chen, Y., Nakamura, R., Bressler, S.L., 2004. Beta oscillations in a large-scale sensorimotor cortical network: directional influences revealed by granger causality. *Proc. Natl. Acad. Sci. U. S. A.* 101, 9849–9854.
- Casali, A.G., Gosseries, O., Rosanova, M., Boly, M., Sarasso, S., Casali, K.R., Casarotto, S., Bruno, M.-A., Laureys, S., Tononi, G., Massimini, M., 2013. A theoretically based index of consciousness independent of sensory processing and behavior. *Sci. Transl. Med.* 5, 198ra105.
- Cauler, L.J., Kulics, A.T., 1991. The neural basis of the behaviorally relevant N1 component of the somatosensory-evoked potential in SI cortex of awake monkeys: evidence that backward cortical projections signal conscious touch sensation. *Exp. Brain Res.* 84, 607–619.
- Del Cul, A., Baillet, S., Dehaene, S., 2007. Brain dynamics underlying the nonlinear threshold for access to consciousness. *PLoS Biol.* 5, e260.
- Engel, A.K., Fries, P., Singer, W., 2001. Dynamic predictions: oscillations and synchrony in top-down processing. *Nat. Rev. Neurosci.* 2, 704–716.
- Ferrarelli, F., Massimini, M., Sarasso, S., Casali, A., Riedner, B.A., Angelini, G., Tononi, G., Pearce, R.A., 2010. Breakdown in cortical effective connectivity during midazolam-induced loss of consciousness. *Proc. Natl. Acad. Sci. U. S. A.* 107, 2681–2686.
- Fetz, E.E., Finocchio, D.V., Baker, M.A., Soso, M.J., 1980. Sensory and motor responses of precentral cortex cells during comparable passive and active joint movements. *J. Neurophysiol.* 43, 1070–1089.
- Hudetz, A.G., Vizuete, J.A., Imas, O.A., 2009. Desflurane selectively suppresses long-latency cortical neuronal response to flash in the rat. *Anesthesiology* 111, 231–239.
- Ito, S., Hansen, M.E., Heiland, R., Lumsdaine, A., Litke, A.M., Beggs, J.M., 2011. Extending transfer entropy improves identification of effective connectivity in a spiking cortical network model. *PLoS One* 6, e27431.
- Jones, E.G., 2001. The thalamic matrix and thalamocortical synchrony. *Trends Neurosci.* 24, 595–601.
- Jones, E.G., Coulter, J.D., Hendry, S.H., 1978. Intracortical connectivity of architectonic fields in the somatic sensory, motor and parietal cortex of monkeys. *J. Comp. Neurol.* 181, 291–347.
- Långsjö, J.W., Maksimow, A., Salmi, E., Kaisti, K., Aalto, S., Oikonen, V., Hinkka, S., Aantaa, R., Sipilä, H., Viljanen, T., Parkkola, R., Scheinin, H., 2005. S-ketamine anesthesia increases cerebral blood flow in excess of the metabolic needs in humans. *Anesthesiology* 103, 258–268.
- Lee, U., Ku, S., Noh, G., Baek, S., Choi, B., Mashour, G.A., 2013. Disruption of frontal–parietal communication by ketamine, propofol, and sevoflurane. *Anesthesiology* 118, 1264–1275.
- Lemon, R.N., 1981. Functional properties of monkey motor cortex neurons receiving afferent input from the hand and fingers. *J. Physiol.* 311, 497–519.
- Lu, J., Nelson, L.E., Franks, N., Maze, M., Chamberlin, N.L., Saper, C.B., 2008. Role of endogenous sleep–wake and analgesic systems in anesthesia. *J. Comp. Neurol.* 508, 648–662.
- Manita, S., Suzuki, T., Homma, C., Matsumoto, T., Odagawa, M., Yamada, K., Ota, K., Matsubara, C., Inutsuka, A., Sato, M., Ohkura, M., Yamanaka, A., Yanagawa, Y., Nakai, J., Hayashi, Y., Larkum, M.E., Murayama, M., 2015. A top-down cortical circuit for accurate sensory perception. *Neuron* 86, 1304–1316.
- Mashour, G.A., 2013. Cognitive unbinding: a neuroscientific paradigm of general anesthesia and related states of unconsciousness. *Neurosci. Biobehav. Rev.* 37, 2751–2759.
- Mashour, G.A., 2014. Top-down mechanisms of anesthetic-induced unconsciousness. *Front. Syst. Neurosci.* 8, 115.
- Muthukumaraswamy, S.D., Shaw, A.D., Jackson, L.E., Hall, J., Moran, R., Saxena, N., 2015. Evidence that subanesthetic doses of ketamine cause sustained disruptions of NMDA and AMPA-mediated frontoparietal connectivity in humans. *J. Neurosci.* 35, 11694–11706.
- Pritchett, D.L., Siegle, J.H., Deister, C.A., Moore, C.I., 2015. For things needing your attention: the role of neocortical gamma in sensory perception. *Curr. Opin. Neurobiol.* 31, 254–263.
- Rivolta, D., Heidegger, T., Scheller, B., Sauer, A., Schaum, M., Birkner, K., Singer, W., Wibral, M., Uhlhaas, P.J., 2015. Ketamine dysregulates the amplitude and connectivity of high-frequency oscillations in cortical–subcortical networks in humans: evidence from resting-state magnetoencephalography-recordings. *Schizophr. Bull.* 41, 1105–1114.
- Rizzolatti, G., Luppino, G., 2001. The cortical motor system. *Neuron* 31, 889–901.
- Rubino, D., Robbins, K.A., Hatsopoulos, N.G., 2006. Propagating waves mediate information transfer in the motor cortex. *Nat. Neurosci.* 9, 1549–1557.
- Saalmann, Y.B., 2014. Intralaminar and medial thalamic influence on cortical synchrony, information transmission and cognition. *Front. Syst. Neurosci.* 8, 83.
- Saleem, K.S., Logothetis, N.K., 2012. A Combined MRI and Histology Atlas of the Rhesus Monkey Brain in Stereotaxic Coordinates. Academic Press.
- Salmi, E., Långsjö, J.W., Aalto, S., Nägren, K., Metsähonkala, L., Kaisti, K.K., Korpi, E.R., Hietala, J., Scheinin, H., 2005. Subanesthetic ketamine does not affect 11C-flumazenil binding in humans. *Anesth. Analg.* 101, 722–725 table of contents.
- Schrouff, J., Perlberg, V., Boly, M., Marrelec, G., Boveroux, P., Vanhaudenhuyse, A., Bruno, M.-A., Laureys, S., Phillips, C., Péligrini-Issac, M., Maquet, P., Benali, H., 2011. Brain functional integration decreases during propofol-induced loss of consciousness. *NeuroImage* 57, 198–205.
- Shipp, S., 2005. The importance of being agranular: a comparative account of visual and motor cortex. *Philos. Trans. R. Soc. Lond. Ser. B Biol. Sci.* 360, 797–814.
- Supér, H., Spekreijse, H., Lamme, V.A.F., 2001. Two distinct modes of sensory processing observed in monkey primary visual cortex (V1). *Nat. Neurosci.* 4, 304–310.
- Tanji, J., Wise, S.P., 1981. Submodality distribution in sensorimotor cortex of the unanesthetized monkey. *J. Neurophysiol.* 45, 467–481.